Article

Evidence of Heritability in Prebiotically Realistic Membrane-Bound Systems

Tymofii Sokolskyi [1,2], Pavani Ganju [1,2], Ronan Montgomery-Taylor [1,2] and David Baum [1,2]*

[1] Wisconsin Institutes for Discovery, University of Wisconsin-Madison, Madison, Wisconsin, 53715
[2] Department of Botany, University of Wisconsin-Madison, Madison, Wisconsin, 53715
* Correspondence: dbaum@wisc.edu;

Abstract: Vesicles of short chain amphiphiles have been demonstrated to grow and divide. Here we explored whether vesicle populations show evidence of heritability. We prepared 1:1 decanoic acid: decylamine vesicles, with or without detergent Triton X-100, in either water or prebiotic soup, a mixture of compounds that might have been present on early Earth. Mixtures were subjected to transfer-with-dilution where, after a 24-hour incubation (one generation), we transferred 10% of the mix into 90% volume of a fresh, vesicle-containing solution. This was continued for 30 generations. Samples with a history of transfers were compared to no-transfer controls (NTCs), initiated each generation using the same solutions but without 10% of the prior generation. We compared the vesicle size distribution and chemical composition of transfer samples and NTCs and compared their fluorescence signal in the presence of Nile Red dye. We observe changes in vesicle size but did not detect differences in chemical composition. In samples with Triton and soup, we observe irregular changes in Nile Red fluorescence, with a tendency for parent and offspring samples to have correlated values, suggestive of heritability. This last result, combined with evidence of temporal autocorrelation across generations, suggests the possibility that vesicles could respond to selection.

Keywords: vesicles; origins of life; evolution; heritability; membranes

Citation: To be added by editorial staff during production.

Academic Editor: Firstname Lastname

Received: date
Revised: date
Accepted: date
Published: date

1. Introduction

Cellular encapsulation is the main mechanism by which extant life maintains concentration gradients and resists environmental stressors, making compartmentalization a key step in the origin of life [1; 2]. The existence of compartments can also facilitate the emergence of adaptive dynamics by constraining parasitic chemical processes [3]. Some models imagine that the first evolvable life was already membrane-bound [2], whereas others imagine encapsulation arising from an earlier mode of spatial organization, for example rock pores [4], mineral surfaces [5; 6], aerosols [7], or coacervate droplets [8; 9]. Whatever the primordial mode of compartmentalization, the cellular habit of all known life shows that vesicles with membranes composed of amphiphilic molecules must have originated very early.

The prebiotic availability of amphiphiles has been questioned [11], but there is evidence to suggest that short and medium chain fatty acids were available on the early Earth [12; 13]. These would have formed during serpentinization [14] or were delivered by extraterrestrial bodies such as meteorites [15; 16] and comets [17].

Vesicles composed of fatty acids can grow by accreting amphiphile molecules and subsequently dividing [18]. This results in autocatalysis, which may help explain the discovery that simple vesicles can have a kind of collective heritability via the "matrix effect" [19]. The matrix effect arises when a small "seed" population of homogeneously sized vesicles is mixed with a much larger population of heterogeneously-sized particles and causes the combined population to acquire a narrow size distribution similar to the seed population. The underlying mechanism is thought to be through a combination of template-directed nucleation and vesicle division dynamics [20; 21]. In addition to the matrix

effect, replicating amphiphile particles, whether micelles or vesicles, can pass information to following generations, encoded in the composition of their amphiphiles and/or associated compounds [22; 10]. Such compositional heritability may allow for natural selection and has been used to suggest that vesicles are capable of adaptive evolution without the need for informational polymers [23; 24].

Our research deploys a recursive seeding (RS) experimental paradigm [25], which resembles experimental evolution protocols for microbial populations (e.g., [26]). In the microbial context, evolution is possible because alternative genotypes can self-replicate, allowing populations to transition to new genotypes as a result of mutation succeeded by drift or selection. By imposing RS on vesicles composed of short chain amphiphiles with or without a mixture of organic compounds as might have been present on early Earth ("prebiotic soup") we aimed to see if analogous phenomena might be observed. This would be supported by showing that there are vesicle traits that change systematically over the course of an RS experiment. Additionally, the RS protocol allows us to look for evidence that trait values in parent and offspring vials are correlated, which would imply some notion of heritability. Such,heritabilitycan be quantified as the fraction of the variation in an offspring generation that can be predicted given the parents.

To characterize populations of vesicles we measure Nile Red fluorescence, which is known to be sensitive to multiple vesicle properties like size, shape and lamellarity. We also estimated particle size distributions using Dynamic Light Scattering (DLS) and tracked overall chemical composition using Liquid Chromatography – Mass Spectrometry (LC/MS). Chemical composition remained constant, but we observed temporal variation in Nile Red fluorescence and vesicle size in the presence of Triton. We also detected evidence of heritability, measured using a linear regression of parent and offspring trait values and temporal autocorrelation of Nile Red fluorescence across generations, but only in the presence of prebiotic soup. Our findings demonstrate the value of the recursive seeding experimental paradigm and suggest the possibility that simple vesicles, interacting with prebiotic soups, have the potential to respond to selection.

2. Materials and Methods

2.1. Vesicle and solution preparation.

The vesicles studied here were made of an equimolar mixture of decanoic acid : decylamine (DA:DN). These prebiotically plausible amphiphiles were chosen due to their ability to produce vesicles under high salt concentrations [28]. For our experiment we incubated vesicles in two different solvents, water and "enriched prebiotic soup" (EPS). EPS is a complex solution consisting of amino acids, nucleobases, cofactors, carboxylic acids and salts adjusted to pH 7 (Table S1), based largely on previous chemical ecosystem selection experiments [29; 16].

To make vesicles, decanoic acid (DA; A765305, VWR International, Hampton, USA) and decylamine (DN; D2404, Sigma Aldrich, St. Louis, USA) were dissolved in 1 mL chloroform to a final concentration of 100 mM, each. A thin film of amphiphiles was generated by evaporating the chloroform under a stream of nitrogen. Then the films were hydrated with 10 mL of either nanopure water or EPS stock solution, to give a final concentration of 10 mM of each amphiphile. Subsequently, the solutions were sonicated for 10 minutes using an FS30 sonicator (Fisher Scientific, Hampton, USA). A 10-minute sonication was chosen based on preliminary data showing that Nile Red fluorescence, which is sensitive to lamellarity, stabilized after 6 minutes of sonication (Fig. S1A). After sonication, samples contained vesicles primarily between 100-500 nm (Fig. S1B).

A subset of vesicle samples was incubated for 24 hours with the detergent Triton X-100 (BP151500, Fisher Scientific, Hampton, USA), which was added immediately prior to incubation to a final concentration of 0.05%. At higher Triton concentrations the only particles detected by our analyses are ~10 nm Triton micelles (see Fig. S6, A). Despite being an unlikely prebiotic compound, Triton X-100 was included since it increases vesicle size

heterogeneity at low concentrations, is non-ionic, and can promote vesicle growth and division [30].

2.2. Recursive seeding design.

We used a recursive seeding (RS) protocol where 10% of the products of the first incubation were introduced as "seed" into a fresh population of vesicles in the next generation (Figure 1). This procedure was repeated for 30 generations, where we compared samples that experienced transfers in their history (TRs) to no-transfer controls (NTCs). NTCs control for differences in reagents and conditions across generations; they use the same vesicle solutions assembled in that generation and were incubated in identical conditions but did not receive a transfer from the previous generation.

The RS experiment was implemented for four treatment categories: 1) EPS, DA:DN; 2) EPS, DA:DN, Triton; 3) Water, DA:DN; 4) Water, DA:DN, Triton. The experiment was conducted with 12 replicates per category per generation in 96-well plates (1185V32, VWR International, Hampton, USA) sealed with plastic covering (15036, VWR International, Hampton, USA) incubated at 25°C in a dark 100 rpm shaking incubator. For TRs, 30 µL of the respective TR from the previous generation was added to 270 µL of the fresh vesicle solution. For NTC solutions, to control for pipetting, 30 µL of the fresh solution was added to a separate batch of 270 µL of the same fresh solution. At the end of the incubation for each generation plates were stored in a -80°C freezer and only thawed immediately prior to conducting analyses. All samples subject to the same kind of analysis were thawed an equal number of times: One thaw for DLS, two for Nile Red fluorescence.

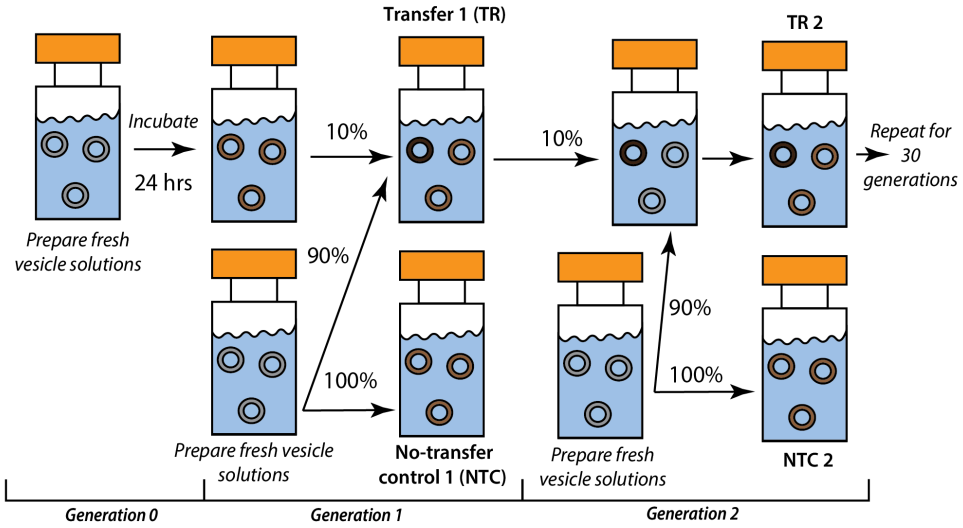

Figure 1. Scheme of the recursive seeding experimental design.

2.3. Nile Red fluorescence measurements.

Nile Red (NR) is a dye that fluoresces in non-polar environments with a fluorescence intensity that is sensitive to a variety of factors [31]. To measure NR fluorescence, we transferred samples to black 96-well plates (37000-550, Thermo Fisher Scientific, Waltham, USA) and added NR (ENZ-52551, Fisher Scientific, Hampton, USA) to each well from a 1 mM stock solution in ethanol, for a final concentration of 0.01 mM. Plates were then placed in a dark 25°C 100 rpm shaking incubator for 1 hour. Subsequently, fluorescence emission at 610, 640 and 660 nm was quantified with a Biotek Synergy HT4 microplate spectrophotometer (Agilent Technologies, Santa Clara, USA) with excitation at 480 nm. Fluorescence intensity was compared between TRs and NTCs with a two-tailed, heteroscedastic t-test.

To look for evidence of heritability, we conducted a linear regression of each TR sample in one generation versus its descendant sample in the next generation. To assess

whether correlation coefficients were more likely to be positive than negative for a given treatment, we used the non-parametric Wilcoxon signed-rank test. To assess longer-term patterns, temporal autocorrelation was assessed using the Statsmodels module in Python [32]. This method determines whether, looking across all generations, the mean value of a given generation is correlated with that found in the preceding generation (lag=1), or the one before that (lag=2), the one before that (lag=3) etc. We only considered lags 1-5, since longer lags are difficult to interpret.

To help with the interpretation of our results, we also determined the effect of 24-hours of incubation on NR fluorescence on Triton-containing samples. We set up 32 replicates and then measured half the samples at the start and half at the end of a 24-hour incubation.

2.4. Dynamic Light Scattering.

Particle size distributions were inferred with dynamic light scattering (DLS) on a Zetasizer Nano (Malvern Pananalytical, Malvern, United Kingdom) with 175° backscattering at 25°C with 3 replicate measurements per sample. The time-resolved correlation function was converted to a hydrodynamic radius versus intensity distribution using the Malvern General Purpose (GP) non-negative least squares distribution fit algorithm with 0.01 regularizer and 70 size classes [33; 34]. As this analysis takes about 4 hours per treatment category in a cuvette reader for a single generation, we analyzed different generations on separate days, but always analyzed TRs and their corresponding NTCs at the same time. To reduce the possibility that time-of-analysis could cause artifactual differences between TR and NTC samples, paired samples were analyzed in an alternate manner (e.g., TR11, NTC11, TR12, NTC12, etc.) Each sample was diluted tenfold in a cuvette with nanopure water immediately prior to measurement to increase DLS resolution, with the exception of EPS samples without Triton, where DA:DN samples were diluted one-hundredfold to minimize interference from a strong peak at around 1 nm, likely representing some kind of a precipitate.

2.5. LC/MS analyses.

For samples not containing Triton (which is incompatible with LC/MS), we analyzed bulk chemical composition using an untargeted metabolomics approach with reverse phase Ultra-Performance Liquid Chromatography coupled with tandem mass-spectrometry (UPLC-MS/MS). Vesicle samples were thawed and immediately diluted 1:10 in LC-grade methanol (A4564, Fisher Scientific, Hampton, USA) and incubated at 25°C with 100 rpm shaking for 1 hour prior to loading on the LC/MS instrument. We used a Thermo Vanquish UPLC (Thermo Fisher Scientific, Waltham, USA) with a C18 column (Agilent, Santa Clara, USA) with 5 μL of samples injected and then eluted in a linear gradient mixture from 0.1% v/v formic acid in water (47146-M6, Thermo Fisher Scientific, Waltham, USA) to 0.1 % v/v formic acid in acetonitrile (47138-K7, Thermo Fisher Scientific, Waltham, USA), over 14 min. To minimize order effects, samples were run with the first replicate of all treatments preceding the second replicate of all treatments, and so on.

The UPLC was coupled to a Thermo Q-Exactive Plus Orbitrap MS (Thermo Fisher Scientific, Waltham, USA). Full MS-SIM spectra for each of the replicates were collected for 10 minutes in positive mode over a scan range of 50–750 m/z, with resolution set to 70000. Fragmentation data were collected only for pooled samples for each treatment category with full MS followed by data-driven MS2 analysis (dynamic exclusion of 4s, intensity threshold 1.0E5, resolution 17500, isolation window 1 m/z, stepped collision energies of 20, 50 and 100 eV). Data files were processed in Compound DiscovererTM (Thermo Fisher Scientific, Waltham, USA), using a default untargeted metabolomics workflow with 16 added databases (Across Organics, Alfa Aesar, Alfa Chemistry, BioCyc, Cambridge Structural Database, CAS Common Chemistry, ChemBank, DrugBank, FDA, Human Metabolome Database, KEGG, MassBank, Merck Millipore, MeSH, NIST, NPAtlas)

and pooled samples set to 'identification only'. Lists of identified compounds and their relative abundances were extracted and differences between TRs and NTCs were evaluated using heteroscedastic t-tests with a Bonferroni alpha correction and principal component analysis plots were produced with Compound DiscovererTM.

3. Results

3.1. Nile Red fluorescence measurements.

In samples without Triton, NR fluorescence at maximum emission wavelength of 640 nm (I_{640}) is minimal and we observed no differences between TRs and NTCs (Figure S2). I_{640} values for NTCs in Triton samples were much higher (Figure S3), having increased significantly over the 24 hours of incubation (Figure S4). There was a high level of variability over generations, suggesting some unidentified source of variation in vesicle preparation. However, since the same batch of vesicles were used for TR and NTC samples, this variation should not invalidate TR:NTC comparisons within generations.

Samples containing Triton demonstrated a significant difference ($p < 0.05$) in NR fluorescence for TRs relative to NTCs for 11 out of 25 measured generations in water, and 6 in EPS (Figure 2, A; Table S2). Significant differences were observed as early as generation 1 in EPS samples. Interestingly, TRs had significantly lower NR fluorescence in generation 1, despite being seeded with a sample (from generation 0) that should, based on the 24 hours incubation data, have started with higher fluorescence (Figure S4). Of the 17 generations with significant differences in either condition, 15 had lower TR than NTC fluorescence. For reasons that are unclear, generation 11 in water was an outlier both in the magnitude and direction of the TR/NTC ratio.

In addition to I_{640}, we calculated the ratio of intensity at 610 nm to 660 nm (I_{610}/I_{660}), which has proven to provide useful information on the polarity of the chemical environment of NR [35, 36]. In both EPS and water samples, I_{610}/I_{660} varied greatly between TR and NTC samples, being significantly ($p<0.05$) different in 11 generations of the EPS lineage and 10 generations in water (Figure 2, B). In 7 of the 11 EPS generations I_{610}/I_{660} is higher in TRs, contrasted with 4 out of 10 generations of water samples.

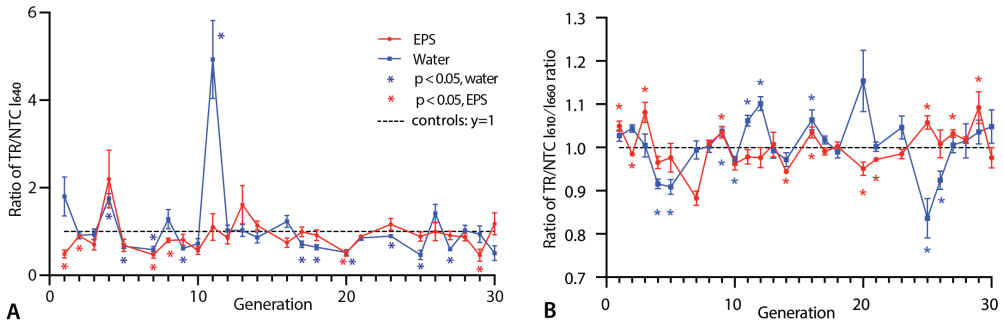

Figure 2. Change in NR fluorescence over generations for samples containing Triton: A – fluorescence intensity with 640 nm emission (I_{640}); B – ratio of intensity at 610 nm to 660 nm (I_{610}/I_{660}). The TR/NTC ratio for each measured generation is shown. Stars mark significant ($p<0.05$) differences between TRs and NTCs as shown by heteroscedastic t-tests on raw TR and NTC values. Error bars are standard errors (12 replicates per measurement).

To determine whether our samples exhibit heritability, we calculated Pearson correlation coefficients for I_{640} between parent and offspring samples within the TR lineages. Results of this test are summarized in Table 1. For EPS samples, we find significant ($p < 0.05$) positive correlation values for four generations in TRs and one generation in NTCs. For water samples, correlation between adjacent generations is mostly negative with 2 generations with significant correlation in NTCs and 3 generations in TRs. Using the non-parametric Wilcoxon's signed-rank test to evaluate the null hypothesis that r-values are

as likely to be positive as negative returns p = 0.056 for all EPS TR pairs or p = 0.040 when samples more than one generation apart (i.e., red values in Table 1) are dropped. While not corrected for multiple tests, this result provides preliminary support for there being some degree of heritability of NR fluorescence (I_{640}) in the presence of EPS. No evidence of heritability was seen for I_{610}/I_{660}.

Given evidence for heritability of I_{640}, we also explored longer-term patterns in TR:NTC ratios (Figure 2, A) over generations using autocorrelation analysis. We find a significant positive autocorrelation for lags 1 and 2 for the EPS samples (Figure S5, A-B). This means that the mean value from a given generation is more similar to the prior two generations than expected by chance. Lags 3 and 4 also showed positive autocorrelation, but this was not significant at lag 3. There was no such pattern of positive autocorrelation for water samples, indeed there was a significant negative autocorrelation for lag 2 (Figure S5, A-B). Analyses based on raw TR values, found significant positive autocorrelation at lag 2 in EPS (Figure S5, E) but NTCs, which have no transfer history, also showed a significantly positive autocorrelation at lag 3 (Figure S5, C).

Table 1. Pearson correlation coefficients (r-values) for I_{640} between parent and offspring generations in the four treatments. Pairs of generations that are more than one generation apart, because the generation in between was not measured, are shown in red. Correlation coefficients with an absolute value greater than 0.3 are bold. Asterisks (*) mark $p < 0.05$. For EPS TR samples, nine of the ten coefficients over 0.3 are positive, including all four significant coefficients.

Generations	Water [NTC]	Water [TR]	EPS [NTC]	EPS [TR]
1-2	-0.18	***-0.62**	**0.43**	-0.09
2-3	0.12	0.01	0.24	***0.65**
3-4	0.00	-0.08	**-0.38**	-0.05
4-5	-0.25	**-0.41**	***0.71**	0.03
5-7	-0.11	0.02	**-0.51**	-0.29
7-8	**0.50**	-0.20	0.04	***0.68**
8-9	**-0.55**	***-0.77**	**0.36**	-0.02
9-10	**-0.50**	**-0.52**	0.17	-0.19
10-11	0.19	**0.42**	**0.30**	***0.58**
11-12	0.04	0.18	-0.01	**0.34**
12-13	-0.14	0.27	0.16	-0.07
13-14	0.01	0.22	0.18	0.17
14-16	**0.39**	-0.06	0.28	**0.47**
16-17	0.29	-0.18	0.06	0.28
17-18	**0.43**	**-0.43**	**0.31**	**0.37**
18-20	0.13	0.11	-0.19	-0.09
20-21	0.04	**-0.57**	-0.27	0.12
21-23	***0.59**	0.13	0.09	**0.31**
23-25	0.43	0.21	-0.22	-0.23
25-26	***-0.58**	-0.04	**-0.52**	**0.32**
26-27	0.14	-0.23	**0.50**	***0.64**
27-28	-0.15	-0.23	-0.15	**-0.35**
28-29	0.24	-0.25	-0.09	0.07
29-30	-0.21	***0.76**	0.09	-0.04
Mean r	0.04	-0.09	0.07	0.15

3.2. Vesicle size measurements.

We monitored vesicle radius change over the course of the experiment using DLS. Freshly-made DA:DN vesicles show a single peak between 100-200 nm that is robust to pH (Figure S6, A). Similarly, pure Triton solutions showed a single peak at 10 nm, presumably representing micelles (Figure S6, B).

Although size-distributions varied considerably, Triton-containing samples often contain particles of two size categories, with modes around 30 nm and 200 nm (Figure 3; Figure S7). In some generations, for example generations 1 and 30 in EPS and generation 9 in water, TRs and NTCs had almost identical size distributions (Figure 3, A, B, E). In other generations TRs and NTCs differed. For example, in generation 11 in water, TR samples have an additional peak between 10-50 nm that is not seen in NTCs (Figure 3, C). This may partially explain why this generation was an outlier for I_{640} (Figure 2, A). In generation 20 in EPS, TRs contain more vesicles in the 90-150 nm size range than NTCs (Figure 3, D). NTCs in generation 30 in water contained more particles <100 nm (Figure 3, E).

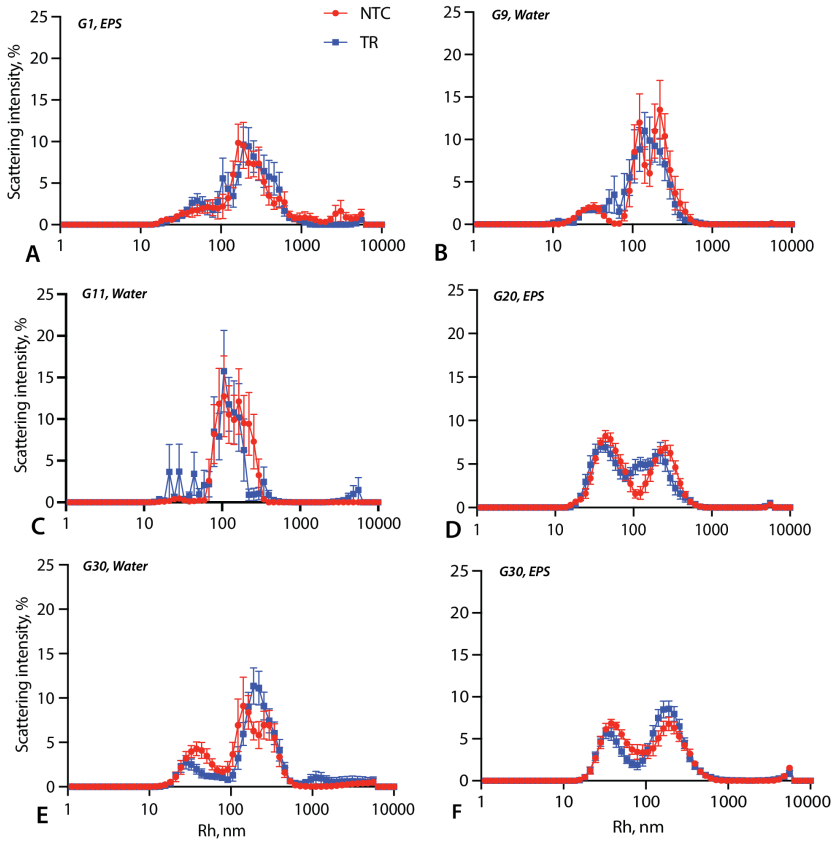

Figure 3. Particle size distributions for samples containing Triton. DLS intensity/hydrodynamic radius distributions are shown for selected generations of EPS (A – generation 1, D – generation 20, F – generation 30) and water (B – generation 9, C – generation 11, E – generation 30). Error bars are standard errors across the 10 replicate samples. Data for other generations are shown in Figure S7.

Samples without Triton showed similarly diverse size distributions (Figure 4) and, again, differences between TRs and NTCs were observed in some generations. In generation 25 in EPS, TR samples included more particles <100 nm (Figure 4, A), whereas there was an excess of particles >1000 nm in generation 30 TRs (Figure 4, B). In water, in both generations 25 and 30, TR size distributions included small peaks below 100 nm that were absent in the NTCs (Figure 4, C, D).

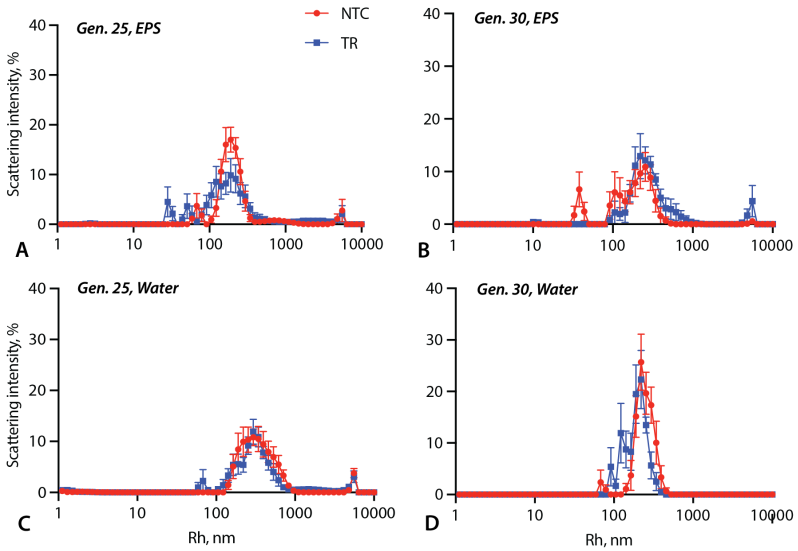

Figure 4. DLS results for samples without Triton. DLS intensity/hydrodynamic radius distributions are shown for selected generations: generation 25, EPS (A) and water (C) and generation 30, EPS (B) and water (D). Error bars are standard errors across 10 replicate samples.

3.3. Chemical composition of EPS samples without Triton.

To understand whether chemical composition of EPS is affected by transfer history, we analyzed TR and NTC samples using LC/MS in generations 25 and 30. Since Triton is incompatible with our LC/MS protocol, only samples without detergent were analyzed. Samples contained several thousands of spectral features identified by Compound Discoverer, with less than 5% being significantly different at $p<0.05$. This result is consistent with TR and NTC samples being compositionally identical. Consistent with this, principal component analysis of the total chemical composition of generation 25 (Figure 5, A-B) and 30 (Figure 5, C-D) samples shows complete overlap between NTCs and TRs.

Since both DA and DN could be detected by LC/MS, we assessed whether these differed measurably between TR and NTC samples. No significant differences were detected (Figure S8).

4. Discussion

4.1. Limitations of the study.

Although we attempted to standardize setup for each generation as much as possible, we still observed marked variation between NTCs from different generations, especially for NR I_{640} (Figure S3). It is unclear whether the intergenerational variation is a result of minor differences in solution preparation or subtle changes in temperature or other environmental variables. One potential source of noise is variation in the duration of freezing. However, although the time that samples spent in the frozen state varied among generations, all samples that were compared to each other (e.g., EPS samples from two different generations) were thawed an equal number of times prior to analysis, which is important because freezing and thawing change membrane dynamics [35]. Moreover, TR and NTC samples from a given generation were always frozen and thawed at the same time.

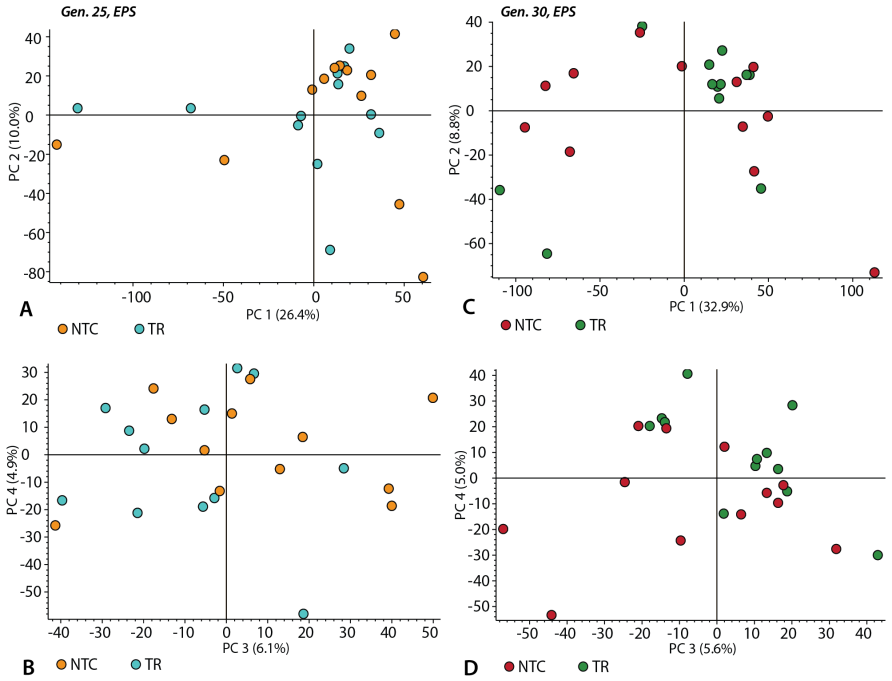

Figure 5. Principal component analysis of the relative abundance of spectral features identified by Compound Discoverer for generation 25, EPS (A, B) and generation 30, EPS (C, D). A, C are plots of principal component (PC) 1 vs PC2; B, D are PC3 vs PC4 (12 replicates per category).

4.2. Explanations for observed patterns.

In this study, we measured vesicle size, chemical composition, and Nile Red fluorescence over the course of multiple generations of RS. Except for chemical composition, we observed multiple cases of significant differences between TR and NTC samples. However, no feature consistently increased or decreased from generation 1 to 30. For example, although I_{640}, which was measured in 25 out of 30 generations, showed a tendency for Triton TRs to have lower values than their corresponding NTCs, this ratio (and the underlying raw values) fluctuated rather than steadily increasing or decreasing.

The observation of a large number of generations in which I_{640} for the Triton samples is significantly lower in TRs than in NTCs cannot be explained by the transfer protocol itself. On the contrary, since I_{640} is higher after vesicles have been incubated for 24-hours (Figure S4), we might have expected TR samples, which receive 90% fresh reagents and 10% previously incubated samples, to have *higher* I_{640} than NTC, which received only fresh reagents. The fact that we saw the opposite pattern suggests that some kind of non-linear vesicle dynamics are triggered by seeding.

NR is a dye that fluoresces in non-polar environments due to twisted intramolecular charge transfer (TICT) between the quinone and diethylamino groups [38] and exhibits different emission peaks based on the solvent [39]. Since NR fluorescence intensity is proportional to the number of NR molecules undergoing TICT, it provides a measure of the abundance of non-polar regions containing NR, which can be affected by many factors including particle size, lamellarity, area/volume ratio, and particle shape [31; 40]. Such complex photophysics is beneficial for our study, as it allows us to track multiple vesicle traits at once without focusing on one specific property.

Although it is possible for changes in I_{640} to result from changes in membrane composition, this is probably not relevant here, since we failed to detect chemical composition differences between samples. Likewise, because we sonicated samples for 10 minutes, whereas just 6 minutes of sonication is sufficient to stabilize I_{640} (Figure S1), changes in lamellarity cannot easily explain TR/NTC differences. Instead, differences in I_{640} are probably due to changes in particle size distributions, including the abundance of micelles.

Pure Triton produces 10 nm micelles (Figure S6, B). However, in the presence of DA:DN lipids, peaks of this size category are absent (Figure 3). This indicates that while micelles may be present, they must be larger (> 30 nm) and include DA and/or DN in addition to Triton. The samples with the smallest DLS size peaks in TRs are from generation 11 in water (Figure 3, C). It may, therefore, not be a coincidence that this generation is an outlier in having significantly greater I_{640} in TR than NTCs (Figure 2, A-B). However, there is no consistent correlation between micelle abundance and reduced fluorescence measurements in TRs.

Interestingly, in addition to I_{640}, the I_{610}/I_{660} ratio is also significantly different between TRs and NTCs in multiple generations. I_{610}/I_{660} can be used to infer micropolarity of a system, with greater values (a stronger blue shift of emission) corresponding to greater burial of NR molecules in hydrophobic structures, such as droplets or bilayers [35, 36]. Differences in micropolarity between TRs and NTCs suggest changes in the abundance of different particle types, only some of which were detectable by DLS analyses. It is difficult to determine which specific types of particles (vesicles, micelles, droplets, etc.) contribute to this dynamic, as I_{610}/I_{660} varies is sensitive to amphiphile identity and concentration. Nonetheless, our data suggest that micropolarity changes significantly over the course of the experiment and appears sensitive to a history of transfers.

In addition to changes in the relative frequency of different aggregates, changes in vesicle size ould explain the lower I_{640} in TRs than in NTCs. As shown in Figure 3, TRs and NTCs differed in particle size distributions in several generations. For example, in generation 20 in EPS there were more larger vesicles in TRs (Figure 3, D), which is consistent with the significantly lower I_{640} in that generation (Figure 2, A). However, the size distributions of generation 30 in water showed a similar pattern without a significant difference in I_{640} (Figure 2, A; Figure 3, E). Similarly, generations 1 in EPS and 9 in water display significantly lower I_{640} fluorescence in TRs but no major difference in DLS results (Figure 2, A; Figure 3, A-B). Thus, while vesicle size distributions and the proportion of micelles likely contribute to different I_{640} levels, it is likely that a multiplicity of factors were responsible for TR-NTC differences, of which changes in shape are worth exploring further in the future. Overall, therefore, it is difficult to assign observed I_{640} dynamics to changes in one specific vesicle property.

4.3. Heritability in vesicle populations.

Vesicles of short chain amphiphiles are known to replicate [18], but it remains uncertain whether this replication process supports the generation of heritable variation that selection could act upon. Here we established RS lineages and looked to see if there was a tendency for samples to inherit characteristics from their parent in the preceding generation. This would be indicated by positive parent-offspring correlations. Additionally, if mean trait values change over time, such heritability would predict a positive autocorrelation in average trait values over generations.

For TRs in water, there is no consistent parent-offspring regression for I_{640}, similar to the pattern seen for NTCs: there are only 2-3 significant correlation coefficients, and these are positive as often as negative, with an average correlation coefficient close to zero. For TRs in EPS, in contrast, there are four significant correlation coefficients, and all are positive. The average correlation over all generations +0.15 (Table 1), which is significantly (or close to significantly) greater than zero depending on whether one includes comparisons that are two generations apart (due to missing samples). Although replication with larger sample sizes is called for, these results suggest the possibility that populations of prebiotically plausible vesicles interacting with EPS are able to express heritable variation upon which selection might be able to act.

This analysis of heritability suggests the possibility of non-genetic inheritance in EPS-Triton samples, but not in the other treatments. If so, and there was also a non-genetic analog of mutation, selection (or mutation bias) could drive directional changes in vesicle populations over generations. Alternatively, we might expect traits to drift over

generations by chance. In either case, we would expect to see temporal autocorrelation where the mean value of a given generation is more similar to its preceding and following generations than to other generations in the RS sequence.

Given that raw I_{640} is sensitive to the mix of vesicles made each generation, which varied greatly (as seen by large fluctuations even in NTCs), autocorrelation analysis is best done on the TR/NTC ratio. We found a significantly positive autocorrelation of ~0.12 in EPS-Triton samples, but a score of ~0 for water samples. Interestingly, this positive temporal autocorrelation extends to generations that are 2, 3, or even 4 apart in the RS sequence of EPS (0.13, 0.09, and 0.30 respectively). These results warrant replication but taken together imply the possibility that EPS-Triton samples may have the capacity for non-genetic evolution.

The matrix effect offers a potential mechanism of heritability that does not require template-based polymerization. However, more experiments and theoretical models would be needed to conclude that this phenomenon is playing a role in vesicle heritability. Given that the effect is only seen in the presence of EPS, compositional inheritance [23; 24] would be a much more plausible explanation.

Interactions of amphiphile assemblies with their chemical environments were emphasized by the Lipid World hypothesis [41]. Models showed that micelles composed of diverse amphiphiles, some of which have catalytic activities, can demonstrate heritability and a response to selection [10; 24]. Similar phenomena could readily occur in vesicle populations due to interactions among diverse, prebiotically plausible amphiphiles [28; 13] and/or amphiphile-induced catalysis of other reactions [42; 43; 44]. Additionally, stochastic encapsulation of solutes, such as "all-or-nothing" encapsulation of proteins [45], could contribute to heterogeneity of populations and could result in heritabilityprovided that chemicals trapped in vesicles show autocatalysis. Models of evolution for systems with compositional inheritance have drawn criticism due to their low replication accuracy [24]. However, in complex systems with multiple distinct components of the membrane and the vesicle lumen, there may be interactions that constrain variation. It is possible, for example, that interactions between compounds in vesicle interior or exterior could stabilize vesicle states in a composition-specific manner [48; 49].

RS experiments are structured in such a way that, if a certain type of vesicle arises that could propagate its characteristics through serial transfer more effectively than other vesicle types, that type would tend to increase in abundance. Thus, even without imposing a conscious selection pressure, the experimental paradigm is capable of inducing adaptive evolution. This may be an explanation for a lack of significant heritability of I_{640} in every generation, since a response to selection often reduces heritability.

Given evidence of heritability of I_{640} even with a 10% transfer fraction, it would be exciting to conduct RS experiments while imposing artificial selection. For example, if there were a way to only seed each generation with those vesicles from the prior generation that resisted a certain environmental challenge, we could then see if resistance to that challenge increased over generations. Adding such direct selection would have the benefit of predicting the direction of the selective response, which should allow for clearer and more definitive statistical tests. The work conducted here provides a valuable baseline for future research, by defining the range of behavior that can be expected even in the absence of intentional selection.

Despite its limitations, this study represents a first attempt to experimentally explore evolution-like dynamics in amphiphilic vesicles. We obtained tentative evidence of heritability and history dependence via temporal autocorrelation, which implies that short chain amphiphile vesicles interacting with complex organic mixtures may show heritability and be capable of adaptive evolution. Although this result warrants replication, ideally utilizing automation to increase sample size and improve replicability, our study illustrates the potential value of RS studies with different amphiphiles and prebiotic soups to shed light on prebiotic evolutionary mechanisms.

Supplementary Materials: The following supporting information can be downloaded at: www.mdpi.com/xxx/s1, Figure S1: Effect of sonication on vesicles; Figure S2: NR fluorescence of generation 25 samples with and without Triton; Figure S3: Raw NR fluorescence of samples with Triton; Figure S4: Impact of incubation on NR fluorescence; Figure S5: Autocorrelation of NR fluorescence; Figure S6: Size of vesicles and micelles; Figure S7: Additional size distributions of samples with Triton; Figure S8: Relative abundance of amphiphiles; Table S1: EPS composition; Table S2: NR fluorescence p-values comparing TRs and NTCs.

Author Contributions: Conceptualization: T.S., D.B.; Methodology: T.S.; Formal analysis: T.S., P.G., R.M.; Writing – original draft preparation: T.S.; Writing – review and editing: T.S., P.G., R.M., D.B.; Supervision – D.B.; Funding acquisition – T.S., D.B.

Funding: This research was funded by the Department of Botany, University of Wisconsin-Madison and NSF Grant DEB 2218817 to DAB.

Data Availability Statement: Raw data generated during this study is available by the following link: https://drive.google.com/file/d/152OdaDBc_2wNW9KTWdivjVoVksFu1tip/view?usp=sharing

Acknowledgments: We would like to thank Daniel Amador-Noguez, Annie Bauer, Betül Kaçar, Zoe Todd, and John Yin for the feedback on this study, Chris Thomas for guidance on LC/MS experiments and data analyses and the labs of Jo Handelsman and John Denu for providing access to plate spectrophotometers. The authors gratefully acknowledge the use of facilities and instrumentation supported by NSF through Wisconsin Materials Research Science and Engineering Center (DMR-1720415) and Anna Kiyanova and Mike Efremov from Soft Material Characterization Lab for providing access and training on the Zetasizer Nano dynamic light scattering instrument.

Conflicts of Interest: The authors declare no conflicts of interest. The funders had no role in the design of the study; in the collection, analyses, or interpretation of data; in the writing of the manuscript; or in the decision to publish the results.

References

1. Ruiz-Mirazo, K., Briones, C., & de la Escosura, A. (2017). Chemical roots of biological evolution: the origins of life as a process of development of autonomous functional systems. *Open biology*, *7*(4), 170050.
2. Monnard, P. A., & Walde, P. (2015). Current ideas about prebiological compartmentalization. *Life*, *5*(2), 1239-1263.
3. Mizuuchi, R., & Ichihashi, N. (2021). Primitive compartmentalization for the sustainable replication of genetic molecules. *Life*, *11*(3), 191.
4. Camprubi, E., Jordan, S. F., Vasiliadou, R., & Lane, N. (2017). Iron catalysis at the origin of life. *IUBMB life*, *69*(6), 373-381.
5. Wächtershäuser, G. (1988). Pyrite formation, the first energy source for life: a hypothesis. *Systematic and Applied Microbiology*, *10*(3), 207-210.
6. Baum, D. A. (2018). The origin and early evolution of life in chemical composition space. *Journal of theoretical biology*, *456*, 295-304.
7. Tuck, A. (2002). The role of atmospheric aerosols in the origin of life. *Surveys in Geophysics*, *23*(5), 379-409.
8. Ghosh, B., Bose, R., & Tang, T. D. (2021). Can coacervation unify disparate hypotheses in the origin of cellular life?. *Current opinion in colloid & interface science*, *52*, 101415.
9. Martin, N., & Douliez, J. P. (2021). Fatty acid vesicles and coacervates as model prebiotic protocells. *ChemSystemsChem*, *3*(6), e2100024.
10. Kahana, A., & Lancet, D. (2021). Self-reproducing catalytic micelles as nanoscopic protocell precursors. *Nature Reviews Chemistry*, *5*(12), 870-878.
11. Deamer, D. W. (2004). Prebiotic amphiphilic compounds. *Origins*, 75-89.
12. Fiore, M., & Strazewski, P. (2016). Prebiotic lipidic amphiphiles and condensing agents on the early Earth. Life, 6(2), 17.
13. Cohen, Z. R., Todd, Z. R., Wogan, N., Black, R. A., Keller, S. L., & Catling, D. C. (2022b). Plausible sources of membrane-forming fatty acids on the early Earth: a review of the literature and an estimation of amounts. *ACS Earth and Space Chemistry*.
14. McCollom, T. M., Ritter, G., & Simoneit, B. R. (1999). Lipid synthesis under hydrothermal conditions by Fischer-Tropsch-type reactions. *Origins of Life and Evolution of the Biosphere*, *29*(2), 153-166.
15. Engel, M. H., & Nagy, B. (1982). Distribution and enantiomeric composition of amino acids in the Murchison meteorite. *Nature*, *296*(5860), 837-840.
16. Vincent, L., Colón-Santos, S., Cleaves, H. J., Baum, D. A., & Maurer, S. E. (2021). The Prebiotic Kitchen: A Guide to Composing Prebiotic Soup Recipes to Test Origins of Life Hypotheses. *Life*, *11*(11), 1221.
17. Dworkin, J. P., Deamer, D. W., Sandford, S. A., & Allamandola, L. J. (2001). Self-assembling amphiphilic molecules: Synthesis in simulated interstellar/precometary ices. *Proceedings of the National Academy of Sciences*, *98*(3), 815-819.
18. Hanczyc, M. M., & Szostak, J. W. (2004). Replicating vesicles as models of primitive cell growth and division. Current opinion in chemical biology, 8(6), 660-664.

19. Blöchliger, E., Blocher, M., Walde, P., & Luisi, P. L. (1998). Matrix effect in the size distribution of fatty acid vesicles. *The Journal of Physical Chemistry B*, *102*(50), 10383-10390.
20. Luisi, P.L., Souza, T.P.D. and Stano, P., 2008. Vesicle behavior: in search of explanations. *The Journal of Physical Chemistry B*, *112*(46), pp.14655-14664.
21. Markvoort, A. J., Pfleger, N., Staffhorst, R., Hilbers, P. A., Van Santen, R. A., Killian, J. A., & De Kruijff, B. (2010). Self-reproduction of fatty acid vesicles: A combined experimental and simulation study. *Biophysical journal*, *99*(5), 1520-1528.
22. Segrè, D., Ben-Eli, D., Deamer, D. W., & Lancet, D. (2001). The lipid world. *Origins of Life and Evolution of the Biosphere*, *31*, 119-145.
23. Segrè, D., Ben-Eli, D., & Lancet, D. (2000). Compositional genomes: prebiotic information transfer in mutually catalytic noncovalent assemblies. *Proceedings of the National Academy of Sciences*, *97*(8), 4112-4117.
24. Vasas, V., Szathmáry, E., & Santos, M. (2010). Lack of evolvability in self-sustaining autocatalytic networks constraints metabolism-first scenarios for the origin of life. *Proceedings of the National Academy of Sciences*, *107*(4), 1470-1475.
25. Baum, D. A., & Vetsigian, K. (2017). An experimental framework for generating evolvable chemical systems in the laboratory. *Origins of Life and Evolution of Biospheres*, *47*, 481-497.
26. Lenski, R. E. (1988). Experimental studies of pleiotropy and epistasis in Escherichia coli. I. Variation in competitive fitness among mutants resistant to virus T4. Evolution, 42(3), 425-432.
27. Kahana, A., Segev, L., & Lancet, D. (2023). Attractor dynamics drives self-reproduction in protobiological catalytic networks. *Cell reports physical science*, *4*(5).
28. Maurer, S. E., Tølbøl Sørensen, K., Iqbal, Z., Nicholas, J., Quirion, K., Gioia, M., Monnard, P.A. & Hanczyc, M. M. (2018). Vesicle self-assembly of monoalkyl amphiphiles under the effects of high ionic strength, extreme pH, and high temperature environments. *Langmuir*, *34*(50), 15560-15568.
29. Vincent, L., Berg, M., Krismer, M., Saghafi, S. T., Cosby, J., Sankari, T., Vetsigian, K., Cleaves, H.J. & Baum, D. A. (2019). Chemical ecosystem selection on mineral surfaces reveals long-term dynamics consistent with the spontaneous emergence of mutual catalysis. *Life*, *9*(4), 80.
30. Noguchi, H. (2013). Structure formation in binary mixtures of lipids and detergents: Self-assembly and vesicle division. *The Journal of chemical physics*, *138*(2), p.01B611.
31. Lin, C., Zhao, J., & Jiang, R. (2008). Nile red probing for the micelle-to-vesicle transition of AOT in aqueous solution. Chemical Physics Letters, 464(1-3), 77-81.
32. Seabold, S., & Perktold, J. (2010). Statsmodels: Econometric and statistical modeling with python. In *Proceedings of the 9th Python in Science Conference* (Vol. 57, No. 61, pp. 10-25080).
33. Stetefeld, J., McKenna, S. A., & Patel, T. R. (2016). Dynamic light scattering: a practical guide and applications in biomedical sciences. *Biophysical reviews*, *8*, 409-427.
34. Chan, M. Y., Dowling, Q. M., Sivananthan, S. J., & Kramer, R. M. (2017). Particle sizing of nanoparticle adjuvant formulations by dynamic light scattering (DLS) and nanoparticle tracking analysis (NTA). *Vaccine Adjuvants: Methods and Protocols*, 239-252.
35. Xu, H., Du, N., Song, Y., Song, S., & Hou, W. (2018). Spontaneous vesicle formation and vesicle-to-micelle transition of sodium 2-ketooctanate in water. *Journal of colloid and interface science*, *509*, 265-274.
36. Sarkar, S., Dagar, S., & Rajamani, S. (2021). Influence of Wet–Dry Cycling on the Self-Assembly and Physicochemical Properties of Model Protocellular Membrane Systems. *ChemSystemsChem*, *3*(5), e2100014.
37. Cohen, Z. R., Todd, Z. R., Catling, D. C., Black, R. A., & Keller, S. L. (2022a). Prebiotic Vesicles Retain Solutes and Grow by Micelle Addition after Brief Cooling below the Membrane Melting Temperature. *Langmuir*, *38*(44), 13407-13413.
38. Sarkar, N., Das, K., Nath, D.N. and Bhattacharyya, K., 1994. Twisted charge transfer processes of nile red in homogeneous solutions and in faujasite zeolite. *Langmuir*, *10*(1), pp.326-329.
39. Teo, W., Caprariello, A.V., Morgan, M.L., Luchicchi, A., Schenk, G.J., Joseph, J.T., Geurts, J.J. and Stys, P.K., 2021. Nile Red fluorescence spectroscopy reports early physicochemical changes in myelin with high sensitivity. *Proceedings of the National Academy of Sciences*, *118*(8), p.e2016897118.
40. Ikari, K., Sakuma, Y., Jimbo, T., Kodama, A., Imai, M., Monnard, P. A., & Rasmussen, S. (2015). Dynamics of fatty acid vesicles in response to pH stimuli. *Soft Matter*, *11*(31), 6327-6334.
41. Segrè, D., Ben-Eli, D., Deamer, D. W., & Lancet, D. (2001). The lipid world. *Origins of Life and Evolution of the Biosphere*, *31*, 119-145.
42. Hitz, T., & Luisi, P. L. (2000). Liposome-assisted selective polycondensation of α-amino acids and peptides. *Peptide Science*, *55*(5), 381-390
43. Zepik, H. H., Rajamani, S., Maurel, M. C., & Deamer, D. (2007). Oligomerization of thioglutamic acid: Encapsulated reactions and lipid catalysis. *Origins of Life and Evolution of Biospheres*, *37*, 495-505.
44. Joshi, M. P., Sawant, A. A., & Rajamani, S. (2021). Spontaneous emergence of membrane-forming protoamphiphiles from a lipid–amino acid mixture under wet–dry cycles. *Chemical science*, *12*(8), 2970-2978.
45. Berclaz, N., Müller, M., Walde, P., & Luisi, P. L. (2001). Growth and transformation of vesicles studied by ferritin labeling and cryotransmission electron microscopy. The Journal of Physical Chemistry B, 105(5), 1056-1064.
46. Lis, L. J., McAlister, D. M., Fuller, N., Rand, R. P., & Parsegian, V. A. (1982). Interactions between neutral phospholipid bilayer membranes. Biophysical journal, 37(3), 657-665.

47. Kim, J. T., Mattai, J., & Shipley, G. G. (1987). Bilayer interactions of ether-and ester-linked phospholipids: dihexadecyl-and dipalmitoylphosphatidylcholines. Biochemistry, 26(21), 6599-6603.
48. Cornell, C.E., Black, R.A., Xue, M., Litz, H.E., Ramsay, A., Gordon, M., Mileant, A., Cohen, Z.R., Williams, J.A., Lee, K.K. and Drobny, G.P. (2019). Prebiotic amino acids bind to and stabilize prebiotic fatty acid membranes. *Proceedings of the National Academy of Sciences*, *116*(35), pp.17239-17244.
49. Todd, Z. R., Cohen, Z. R., Catling, D. C., Keller, S. L., & Black, R. A. (2022). Growth of prebiotically plausible fatty acid vesicles proceeds in the presence of prebiotic amino acids, dipeptides, sugars, and nucleic acid components. *Langmuir*, *38*(49), 15106-15112.

Supplementary Information Appendix

Evidence of heritability in prebiotically realistic membrane-bound systems

Tymofii Sokolskyi[1,2], Pavani Ganju[1,2], Ronan Montgomery-Taylor[1,2], David Baum[1,2]

1 – Wisconsin Institutes for Discovery, University of Wisconsin-Madison, Madison, Wisconsin, 53715

2 – Department of Botany, University of Wisconsin-Madison, Madison, Wisconsin, 53706

Enriched Prebiotic Soup (EPS) preparation

Compounds in concentrations listed in Table S1, with the exceptions of ammonium persulfate (APS) and sodium trimetaphosphate (TMP), were mixed in a glass beaker and then dissolved in 1L of water with stirring. Resulting solution was dispensed into 50 mL plastic tubes and stored at -20°C until use. Immediately prior to experimental use, EPS stocks were thawed, filtered through a 200 nm syringe filter (431215, DOT Scientific Inc., Burton, USA) and TMP and APS were added to appropriate final concentrations.

Compound	Class	Vendor	CAS #	Final Concentration (mM)
1,3-dihydroxyacetone	Triose	Fisher Scientific	96-26-4	0.32
2-aminobutyric acid	Amino Acid	Acros Organics	2835-81-6	0.08
acetic acid	Organic Acid	Sigma-Aldrich	?	0.32
acetoguanamine	Triazine	VWR	541-02-9	0.16
adenine	Nucleobase	Fisher Scientific	73-24-5	0.32
ammonium chloride	Salt/Redox Energy	Sigma-Aldrich	12125-02-9	20
ammonium persulfate**	Salt/Oxidant	IBI Scientific	7727-54-0	0.04
butyric acid (sodium salt)	Organic Acid	Fisher Scientific	156-54-7	0.08
cobalt(II) chloride anhydrous	Transition Metal Salt	BTC Chemicals	7646-79-9	0.001
copper(II) chloride dihydrate	Transition Metal Salt	Alfa Aesar	10125-13-0	0.001
cytosine	Nucleobase	Fisher Scientific	71-30-7	0.32
D-(-)-ribose	Monosaccharide	Fisher Scientific	50-69-1	0.16
D-(+)-xylose	Monosaccharide	Fisher Scientific	58-86-6	0.16
D-glucose	Monosaccharide	DOT Scientific Inc.	54-99-7	0.16
DL-arabinose	Monosaccharide	VWR	147-81-9	0.16
formic acid 90%	Organic Acid	Aqua Solutions	64-18-6	0.64
glycerol	Trihydric Alcohol	DOT Scientific Inc.	56-81-5	0.32
glycolic acid	α-Hydroxy Acid	Acros Organics	79-14-1	0.32
hydroxybutyric acid	β-Hydroxy Acid	Sigma-Aldrich	150-83-4	0.08
iminodiacetic acid	Dicarboxylic Acid Amine	VWR	142-73-4	0.16
L-alanine	Amino Acid	VWR	56-41-7	0.32
L-arginine	Amino Acid	Sigma-Aldrich	74-79-3	0.16

L-ascorbic acid	Reducing Agent/Co-factor	DOT Scientific Inc.	50-81-7	0.04
L-asparagine	Amino Acid	Acros Organics	5794-13-8	0.16
L-aspartic acid	Amino Acid	Alfa Aesar	56-84-8	0.32
L-cysteine	Amino Acid	DOT Scientific Inc.	52-90-4	0.16
L-glutamic Acid	Amino Acid	VWR	56-86-0	0.32
L-glutamine	Amino Acid	Sigma-Aldrich	56-85-9	0.16
L-glycine	Amino Acid	Sigma-Aldrich	54-40-6	0.32
L-histidine	Amino Acid	DOT Scientific Inc.	71-00-1	0.08
L-isoleucine	Amino Acid	DOT Scientific Inc.	73-32-5	0.16
L-leucine	Amino Acid	DOT Scientific Inc.	61-90-5	0.32
L-lysine	Amino Acid	DOT Scientific Inc.	657-27-2	0.32
L-methionine	Amino Acid	DOT Scientific Inc.	63-68-3	0.08
L-phenylalanine	Amino Acid	DOT Scientific Inc.	63-91-2	0.16
L-proline	Amino Acid	Alfa Aesar	147-85-3	0.16
L-serine	Amino Acid	DOT Scientific Inc.	56-45-1	0.32
L-threonine	Amino Acid	DOT Scientific Inc.	72-19-5	0.32
L-tryptophan	Amino Acid	DOT Scientific Inc.	73-22-3	0.08
L-tyrosine	Amino Acid	Amresco	60-18-4	0.16
L-valine	Amino Acid	DOT Scientific Inc.	72-18-4	0.32
lactic acid 88% solution	α-Hydroxy Acid	Fisher Scientific	50-21-5	0.16
magnesium chloride	Sea Salt	DOT Scientific In.	7791-18-6	50
N-ethanolamine	Amino Alcohol	Sigma-Aldrich	141-43-5	0.08
N-methylalanine	Amino Acid	Sigma-Aldrich	3913-67-5	0.08
N-methylglycine	Amino Acid Derivative	Acros Organics	107-97-1	0.16
N-methylurea	Amide	Fisher Scientific	759-73-9	0.08
nicotinamide	Cofactor	DOT Scientific Inc.	98-92-0	0.08
potassium chloride	Sea Salt	VWR	7447-40-7	10

propionic acid	Organic Acid	Fisher Scientific	79-09-4	0.16
pyruvic acid	α-Keto Acids	Fisher Scientific	127-17-3	0.08
R-pantetheine	Cofactor	Sigma-Aldrich	496-65-1	0.04
sodium bisulfite	Reducing agent	Ward's	7631-90-5	0.08
sodium chloride	Sea Salt	Fisher Scientific	7647-14-5	500
sodium molybdate	Transition Metal Salt	Strem Chemicals	10102-40-6	0.001
sodium nitrate	Salt	Sigma-Aldrich	7631-99-4	20
succinic acid	Dicarboxylic Acid	Sigma-Aldrich	110-15-6	0.08
succinonitrile	Nitrile	VWR	110-61-2	0.16
thymine	Nucleobase	Fisher Scientific	65-71-4	0.32
trisodium trimetaphosphate**	Phosphate Source	Sigma-Aldrich	7785-84-4	0.1
uracil	Nucleobase	VWR	66-22-8	0.32
urea	Amide	IBI Scientific	57-13-6	0.16
zinc(II) chloride	Transition Metal Salt	Sigma-Aldrich	7646-85-7	0.001
β-alanine	Amino Acid	Tokyo Chemical	107-95-9	0.32
iron (II) chloride	Transition Metal Salt	Alfa Aesar	7758-94-3	0.001
manganese (II) sulfate monohydrate	Transition Metal Salt	Sigma-Aldrich	7487-88-9	0.001

Table S1. EPS composition. ** indicates compounds that were added immediately prior to use (TMP and APS).

Effect of sonication time on vesicle size and NR fluorescence. To test whether vesicle lamellarity is a contributing factor to changes in NR fluorescence and size, we measured vesicle solutions in water without Triton, sonicated for different times. Since sonication time is expected to be inversely proportional to lamellarity (Maurer et al., 2018), we predicted a decline in NR fluorescence with sonication. As predicted, NR fluorescence drops after ~4 minutes of sonication and remains stable for the duration of the time-course (**Fig. S1, A**). Similarly, vesicle size distribution of unsonicated vesicles suggests a larger size than vesicles sonicated for 10 minutes (**Fig. S1, B**).

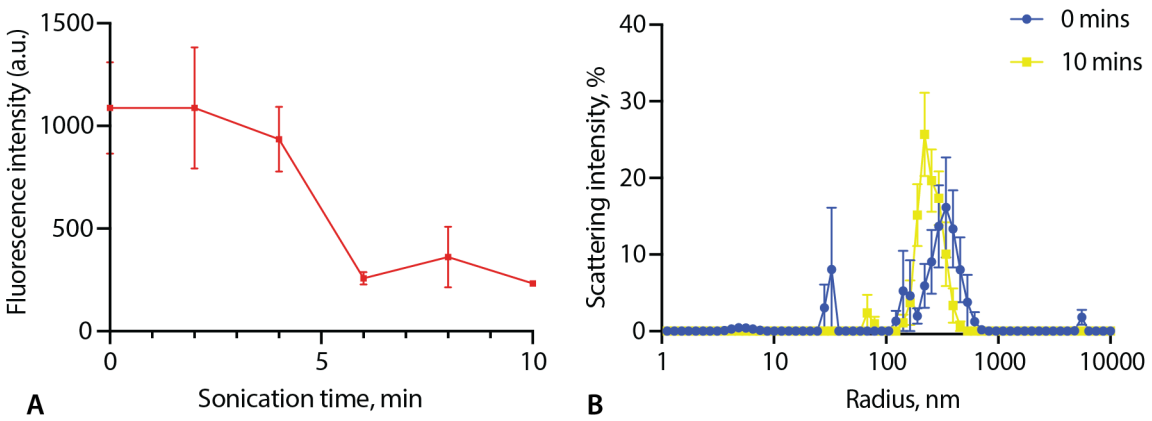

Figure S1. Results of the 10 minute sonication test on vesicles composed of 20 mM 1:1 DA:DN in water. **A** – Nile Red fluorescence intensity over sonication time; **B** – size distributions of unsonicated and sonicated vesicles. Error bars are standard error (12 replicates for **A**, 3 replicates for **B**).

Generation	EPS	Water
1	0.00055171	0.153476769
2	0.00491489	0.579675521
3	0.16115933	0.6836678
4	0.11314095	0.002685796
5	0.21314719	0.000592203
7	0.00855078	0.007956636
8	0.009686	0.381839385
9	0.17410591	2.91172E-07
10	0.17949402	0.095197113
11	0.76135622	0.001002305
12	0.41611784	0.866752562
13	0.21922503	0.886798447
14	0.31832474	0.379641724
16	0.09234096	0.286683154
17	0.9716847	0.020788254
18	0.55434033	0.001030556
20	0.00183984	0.044239599
21	0.07552436	0.099381047
23	0.27278224	0.049111401
25	0.39111247	0.007031338
26	0.99117549	0.104085514
27	0.59941244	0.000388879
28	0.41574193	0.903164937
29	0.00295851	0.793949012
30	0.59977185	0.115396303

Table S2. p-values derived from a two-tailed heteroscedastic t-test comparing raw NTC and TR NR fluorescence intensity values of samples containing Triton X-100 in either EPS or water.

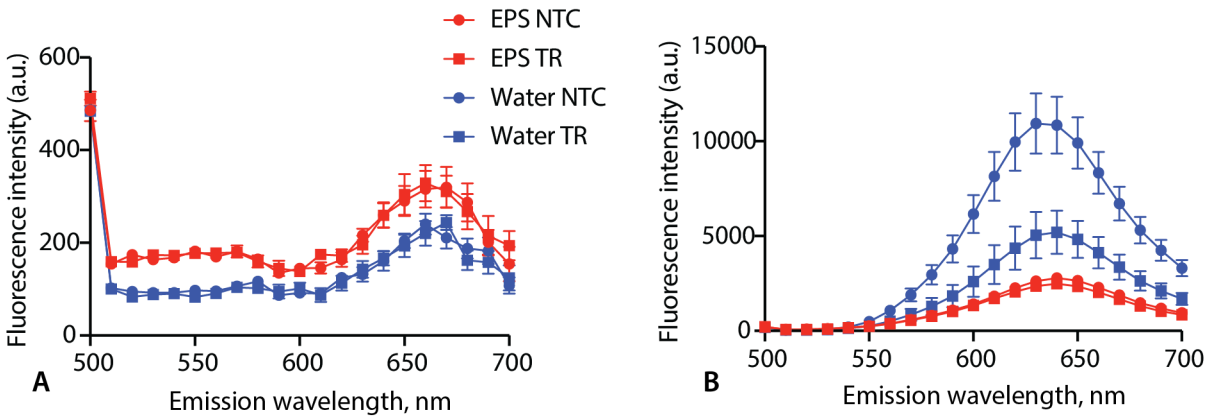

Figure S2. Comparison between Nile Red fluorescence emission spectra with 480 nm excitation wavelength for samples without (**A**) and with (**B**) Triton X-100 at generation 25. Note extremely low fluorescence of samples without the detergent. Error bars are standard error (12 replicates).

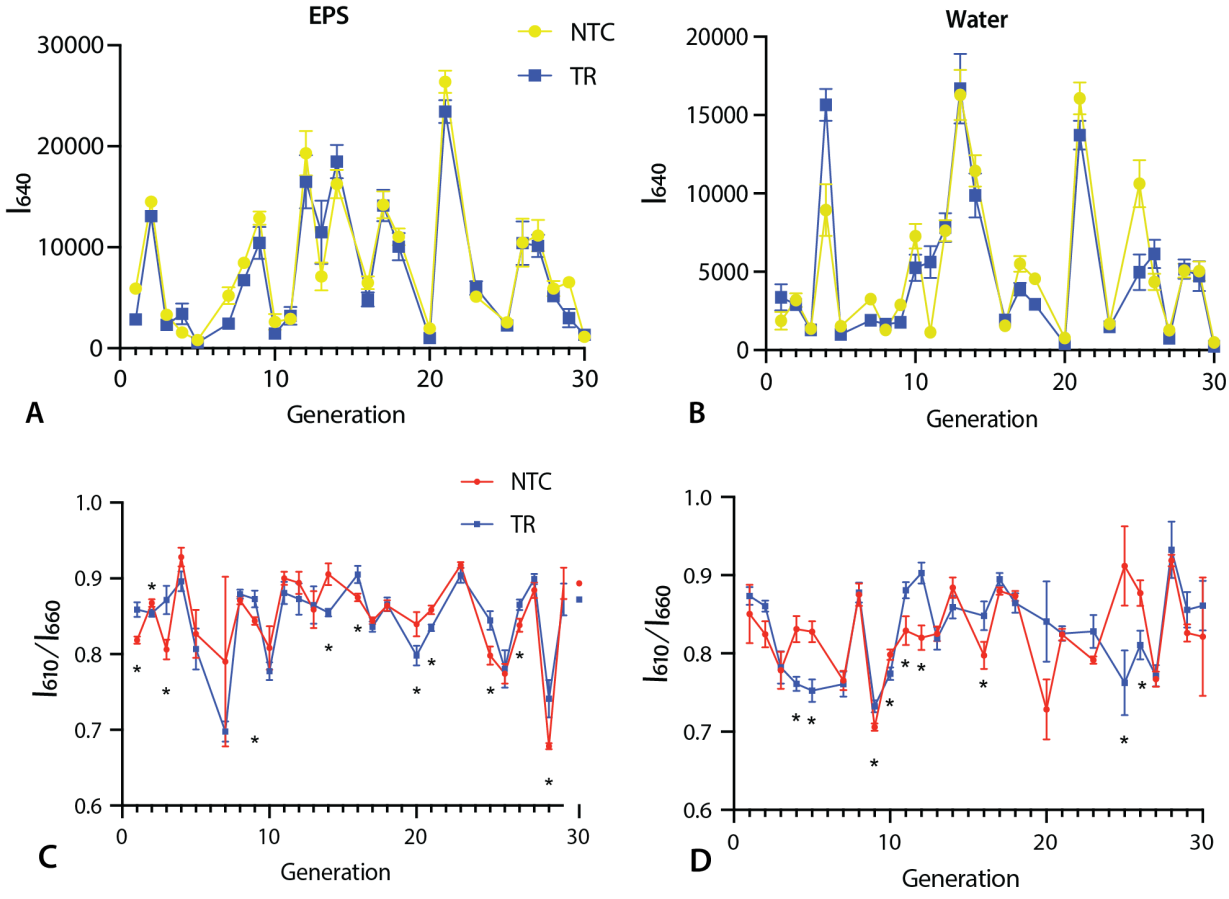

Figure S3. Raw NR fluorescence intensity plots for NTCs and TRs of EPS and water samples with Triton. **A** – I_{640} for EPS samples over 30 generations; **B** – water samples; **C** – I_{610}/I_{660} for EPS; **D** – I_{610}/I_{660} for water. Error bars are standard error (12 replicates).

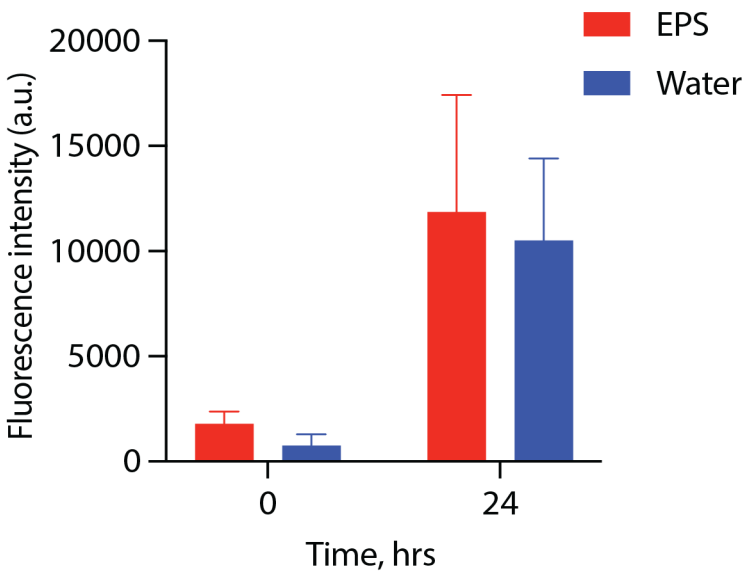

Figure S4. Comparison between Nile Red fluorescence emission spectra with 480 nm excitation and 640 nm emission wavelengths for 20 mM 1:1 DA:DN with 0.05% Triton samples incubated in water or EPS for 0 and 24 hours. Error bars are standard error (16 replicates).

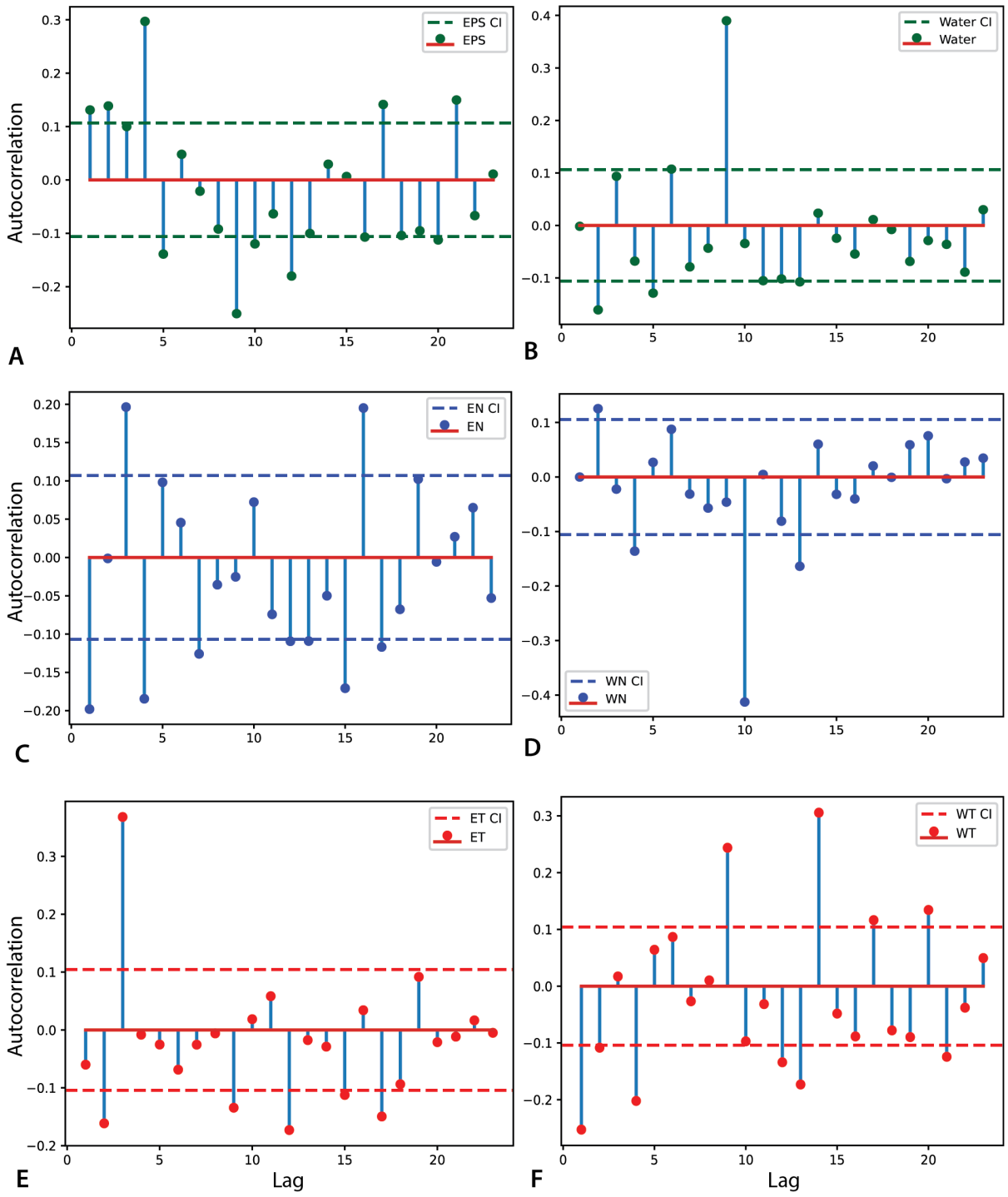

Figure S5. Autocorrelation function (ACF) values for the 12-replicate Triton samples over 25 generations with 95% confidence intervals. **A–B**: ACF plots for the NR fluorescence TR/NTC ratios of EPS (**A**) and water (**B**) samples; **C–F**: ACF plots for the raw NR Fluorescence of EPS NTCs (**C**), Water NTCs (**E**), EPS TRs (**E**), and Water TRs (**F**). Python code for this analysis is attached separately.

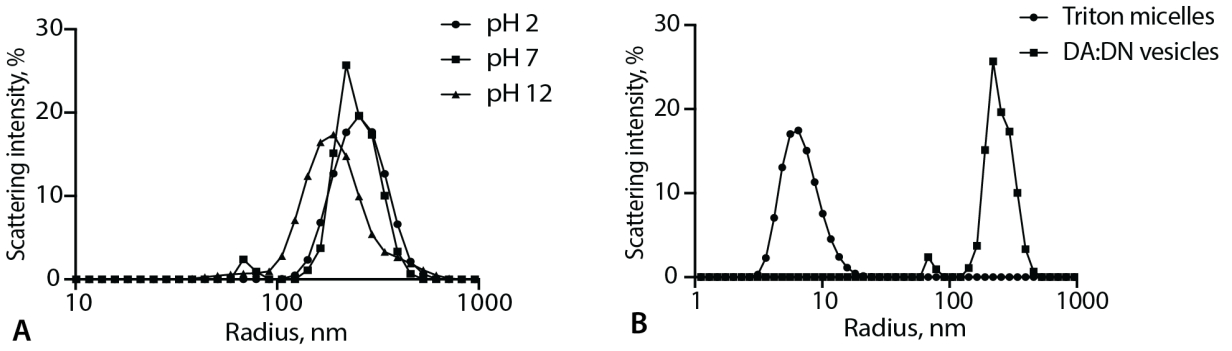

Figure S6. A – size distributions of 20 mM 1:1 DA:DN vesicles at pH 2, 7 and 12 that demonstrates lack of micelles or large particles in acidic and basic samples (1 replicate). **B** – comparison between the sizes of pure 0.05% Triton X-100 micelles and DA:DN vesicles (1 replicate).

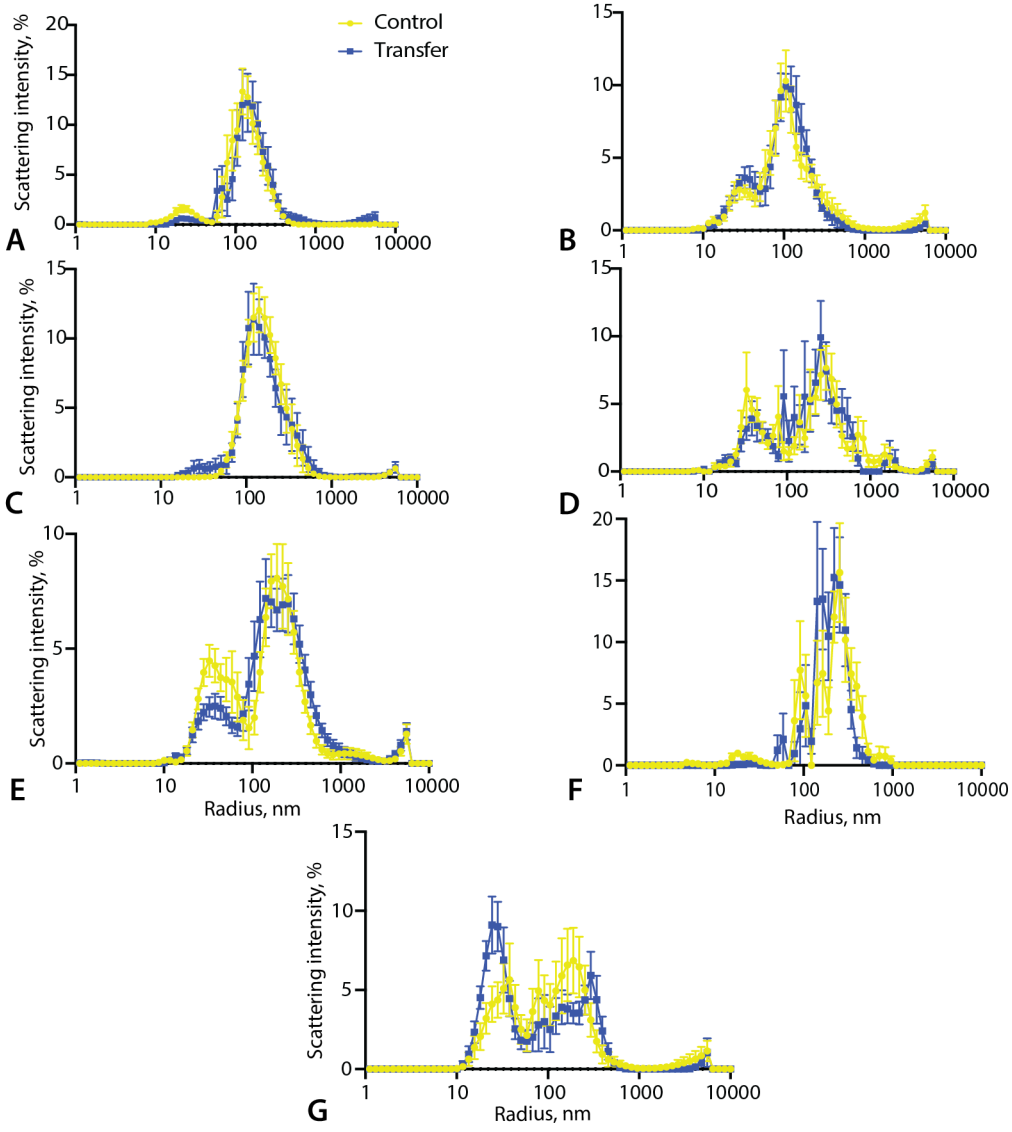

Figure S7. Size distributions of samples containing Triton X-100: **A** – generation 5, EPS; **B** – generation 5, water; **C** – generation 10, EPS; **D** – generation 10, water; **E** – generation 20, water; **F** – generation 25, EPS; **G** – generation 25, water. Error bars are standard error (10 replicates).

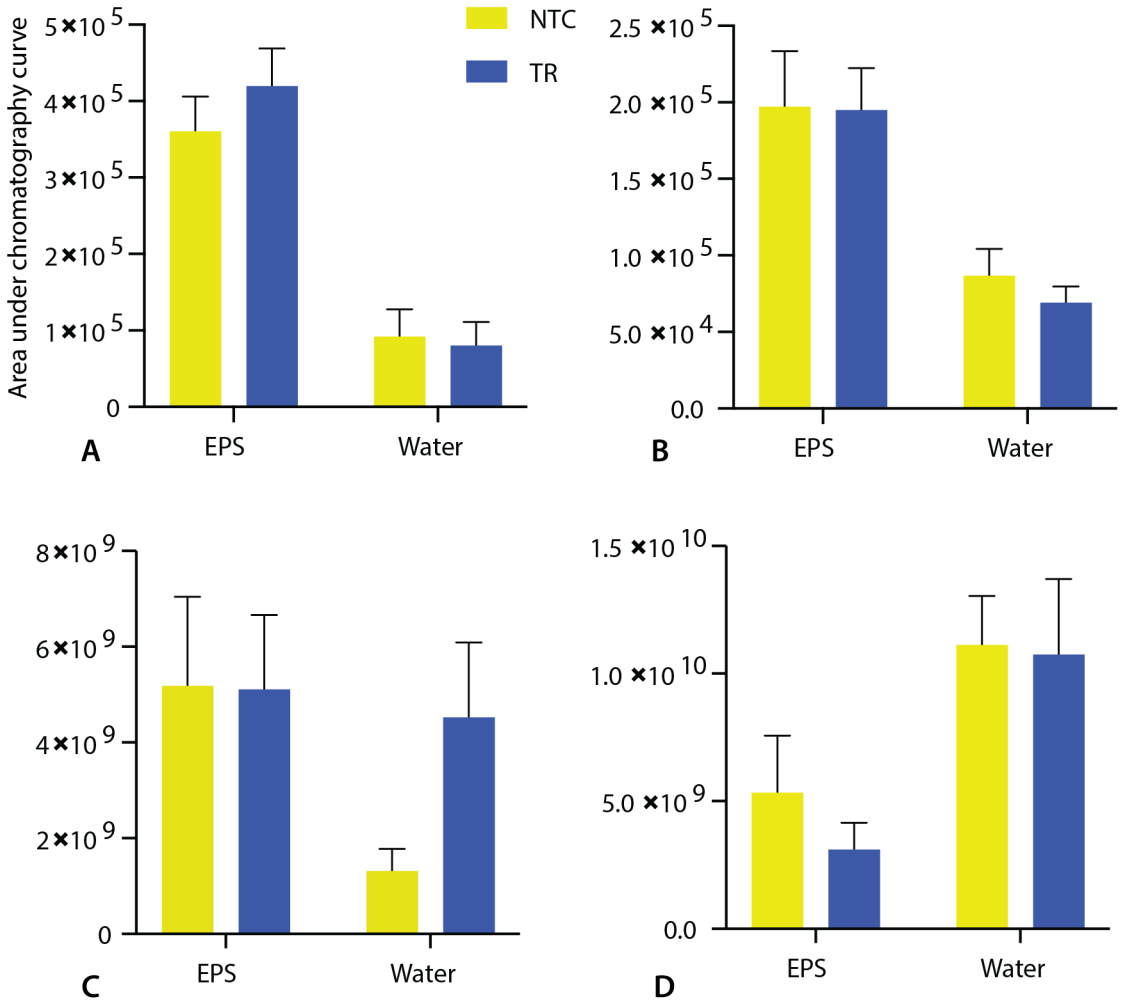

Figure S8. Relative abundance of amphiphiles as measure by LC peak area under the curve for samples without Triton X-100. **A** – DA, generation 25; **B** – DA, generation 30; **C** – DN, generation 25; **D** – DN, generation 30. No significant differences between TRs and NTCs are observed. Error bars are standard error (12 replicates).